Journal of Alloys and Compounds 504 (2010) 503–507

Contents lists available at ScienceDirect

Journal of Alloys and Compounds

journal homepage: www.elsevier.com/locate/jallcom

Preparation, characterization and properties of thermochromic tungsten-doped vanadium dioxide by thermal reduction and annealing

Junwei Ye[a], Li Zhou[a], Fengjuan Liu[a], Ji Qi[b], Weitao Gong[a], Yuan Lin[a], Guiling Ning[a,*]

[a] State Key Laboratory of Fine Chemicals and School of Chemical Engineering, Dalian University of Technology, 158 Zhongshan Road, Dalian 116012, PR China
[b] Department of Chemical Engineering, Dalian Nationalities University, 18 Liaohe West Road, Dalian 116600, PR China

ARTICLE INFO

Article history:
Received 19 March 2010
Received in revised form 27 May 2010
Accepted 29 May 2010
Available online 11 June 2010

Keywords:
Vanadium oxide
Tungsten
Doping
Thermal reduction

ABSTRACT

Thermochromic tungsten-doped vanadium dioxide (VO_2) powders were successfully synthesized by thermal reduction using V_2O_5 as a vanadium precursor. The products were characterized by X-ray diffraction (XRD), X-ray photoelectron spectroscopy (XPS), scanning electron microscopy (SEM) and differential scanning calorimetry (DSC). The results indicated that W was successfully doped into the crystal lattice of VO_2 matrix, and prepared tungsten-doped VO_2 had a rod-like morphology. The effects of reducing temperature and annealing temperature on the crystallographic structures were also discussed. The phase transition temperature (Tt) of VO_2 could be simply tuned by changing the doping concentration of tungsten. When the doping concentration was 1.58 mol%, the Tt could be reduced to 37.8 °C from initial 69.5 °C, suggesting that tungsten-doped VO_2 possesses prominent thermochromic properties and optical switching characters. It has shown that this convenient and efficient approach could be applied in the mass-production of functional powders materials.

1. Introduction

Over the past decade, vanadium oxide compounds have attracted increasing attention because of their unique properties and potential applications in catalysis, optical, optoelectronic and electrochemical devices [1–5]. Among the various vanadium oxide compositions, vanadium dioxide (VO_2) exhibits a reversible semiconductor–metal phase transition when it undergoes a crystallographic structure transformation from monoclinic $P2_1/c$ to tetragonal $P4_2/mnm$ at about 68 °C [6,7], involving variations in magnetic, electrical and optical properties [8,9]. These features make VO_2 suitable for applications in near-infrared optical switches, smart window coatings, temperature-sensing devices and data storage mediums [10–12].

Up to now, various micro- and nano-structures of VO_2, such as ribbons, belts, rods, wires, microspheres and thin film, have been prepared by different methods. These methods include chemical vapor deposition, magnetron sputtering, vacuum evaporation, high-energy ion beam implantation, etc. [13–17]. Baudrin et al. prepared VO_2 filaments by heating vanadium oxide aerogels under vacuum [13]. Li et al. synthesized VO_2 nano-belts by a hydrothermal reaction between oxalic acid and V_2O_5 [14]. Xie and co-workers reported a new method to obtain VO_2 by direct combustion of an solution of $VO(acac)_2$ in a confined space [15]. Liu and co-workers prepared VO_2 micro-blocks by chemical vapor deposition using $VO(acac)_2$ as a vanadium precursor [16]. Su and co-workers reported a facile template-free approach to prepare hollow VO_2 microspheres [17]. Most of the reported methods inevitably need either expensive equipments or exact conditional parameters, which have some difficulties and complexities in controlling the oxidation state of vanadium of final products. Furthermore, the higher phase transition temperature (Tt) of VO_2 confines its extending applications in intelligent window coating, and tuning of Tt to nearly room temperature becomes one of the research focuses. It has been proved that doping with high-valence metal ions into the VO_2 lattice is an effective way to decreasing the Tt [18,19]. Recently, more effort has been devoted to developing new approaches to preparing doped VO_2 powders with adjustable Tt [20–23]. For examples, Cao et al. synthesized tungsten (W)-doped VO_2 via the hydrothermal reaction of V_2O_5, oxalic acid and tungstenic acid [20]. Peng et al. reported the synthesis of W-doped VO_2 nanopowders by thermolysis of $(NH_4)_5(VO)_6(CO_3)_4(OH)_{10}\cdot 10H_2O$ [21]. It is still a great challenging to simply and inexpensively obtain the doped VO_2 powders in real large quantities.

In this paper, we reported a simple thermal reduction technique to prepare W-doped VO_2 powders using tungsten acid as the dopant. The effects of experimental parameters on the formation of the product were investigated in detail. And the

---

[*] Corresponding author. Tel.: +86 411 39893609; fax: +86 411 39893609.
E-mail address: ninggl@dlut.edu.cn (G. Ning).

0925-8388/$ – see front matter © 2010 Elsevier B.V. All rights reserved.
doi:10.1016/j.jallcom.2010.05.152

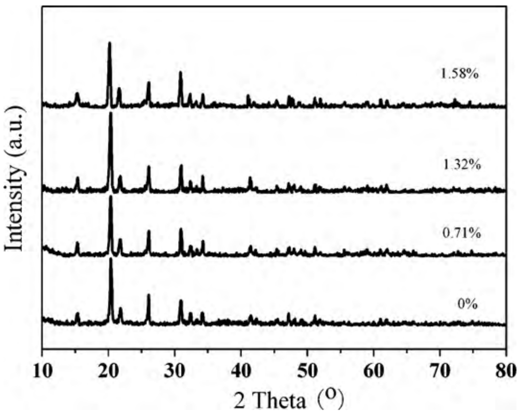

Fig. 1. XRD patterns of the W-doped V_2O_5 precursors with different W-doping fractions (mol%).

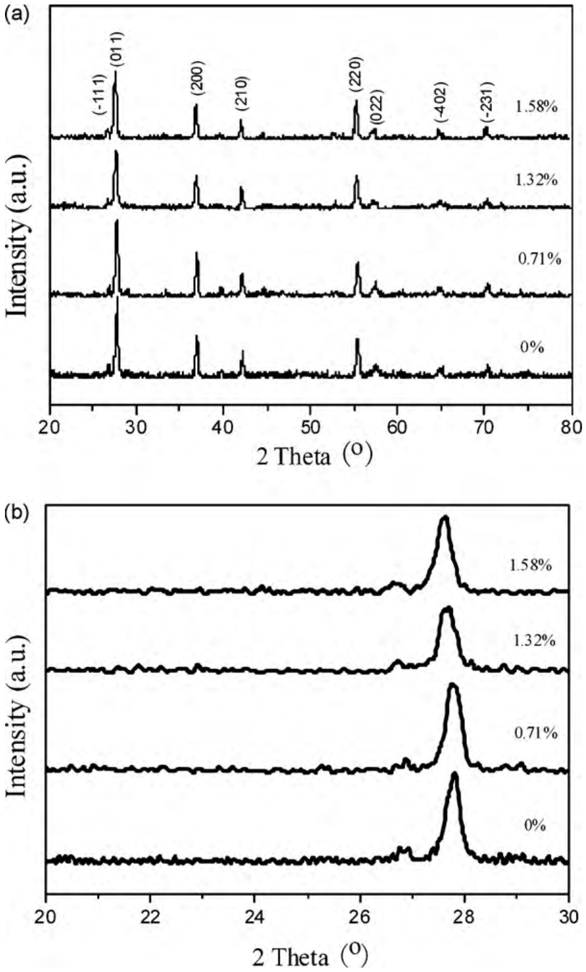

Fig. 2. XRD patterns of W-doped VO_2 with different W-doping fractions (mol%): normalized (a) and magnified (b) patterns.

morphology, structure and properties of products were also presented.

2. Experimental

2.1. Preparation of W-doped VO_2

All chemicals are commercially available and used as received without further purification. In a typical experiment, V_2O_5 (2.00 g) and tungsten acid (0.05 g) were mixed and put into a ceramic crucible. The mixture was then heated to 800 °C in an electric furnace for about 20 min. When a molten liquid was formed, the mixture was quickly poured into distilled water (100 mL) to give brownish W-doped V_2O_5 sol. After evaporating at 70 °C, amorphous W-doped V_2O_5 dried gel was obtained. Then polycrystalline particles of precursor W-doped V_2O_5 were collected by calcination of dried gel at 400 °C for 1 h. Reduction of the precursor W-doped V_2O_5 to W-doped VO_2 was carried out according to our previously reported procedure [24], i.e. W-doped V_2O_5 particles were heated under mixed gas flow of ammonia (NH_3, 15 mL/min) and nitrogen (N_2, 150 mL/min) at 500 °C for 1 h, and further annealed in N_2 at 650 °C for 5 h. At last, dark blue powder products were synthesized. The effects of atomic percentages of V and W, reduction and annealing temperatures on the preparation were investigated in detail. The samples obtained under different conditions were denoted as a–e (Table 1).

2.2. Characterizations

The crystal structures of the as-prepared samples were characterized by powder X-ray diffraction (XRD) on a Rigaku D/max 2400 X-ray equipped with graphite monochromatized Cu Kα radiation ($\lambda = 1.5406$ Å). A scan rate of 0.02° s^{-1} was applied to record the pattern in the 2θ range from 10° to 70°. The size and morphology of samples were observed on scanning electron microscopy (SEM, JEOL-5600 LV) at an acceleration voltage of 15.0 kV. Valences of the elements were studied by X-ray photoelectron spectroscopy (XPS, VG ESCALAB MK II). DSC 204 (Netzsch, Germany) was used to measure the thermal properties of samples at a heating rate of 10 K/min in ultrapure nitrogen atmosphere. IR spectra were measured by a spectrometer (AVATAR370, Thermo Nicolet, America) equipped with a temperature-control apparatus.

3. Results and discussion

The crystal structure and phase purity of the as-prepared products were determined by XRD. Fig. 1 shows XRD patterns of the as-prepared precursors with different W-doping fractions. It indicated that the obtained precursor powders are well crystalline V_2O_5 (JCPDS Card No. 72-0433) and no other vanadium oxides are observed. By reduction of precursor in a reducing atmosphere, the thermochromic W-doped VO_2 products could be obtained. The XRD patterns of the obtained W-doped VO_2 samples with different W fractions synthesized by heating at 550 °C for 1 h and annealing at 700 °C for 5 h are shown in Fig. 2a. All typical diffraction peaks can be indexed to VO_2 (M) phase (JCPDS Card No. 44-0252, $P2_1/c$, $a = 4.506$ Å, $b = 2.899$ Å, $c = 4.617$ Å and $\beta = 91.79°$) and impurities phase cannot be found in the samples. And the peaks belong to WO_3 are not observed because of doping W into vanadium oxide as the solute donor [25], which indicated that W enter into the crystal lattice of VO_2 matrix. In addition, it is also observable that most peaks of doped VO_2 samples shift slightly towards lower 2θ value (Fig. 2b). It is well known that the ionic radius of W is larger than of V, so when W atoms substitute V atoms in VO_2 lattice, adjacent interplannar distance $d_{(hkl)}$ becomes larger, resulting in the peaks shift toward low 2θ angle.

Our experiments show that the process for the preparation of W-doped VO_2 (M) phase involves an intermediate step, in which allotropic phase VO_2 (B) forms [26]. XRD patterns of the samples obtained on different conditions (Table 1) are shown in Fig. 3, which indicates that samples exhibited crystal phase transformation from VO_2 (B) to thermochromic VO_2 (M) phase as the heat treatment temperature heightened. Fig. 3a displays the XRD patterns of the obtained samples by heating at 500 °C for 1 h, we can observe obvious diffraction peaks according to VO_2 (B) (JCPDS No. 81-2392). When heating temperature is 550 °C for 1 h and annealing temperature is 600 °C for 5 h, all peaks index VO_2 (M). Furthermore, all peaks became stronger and narrower when annealing temperature is enhanced, suggesting that larger crystal is formed at higher temperature. The transformation from VO_2 (B) to VO_2 (M) is a crucial step to prepare thermochromic materials because VO_2 (B) does not possess reversible phase transition property. Therefore required reduction and annealed temperature are 500–550 and 650–700 °C, respectively for the preparation of thermochromic W-doped VO_2.

Valence analysis of the obtained W-doped VO_2 sample was investigated by the typical XPS spectrum as shown in Fig. 4, which

Table 1
Synthesis conditions for different samples.

Samples	Reduction condition		Annealing condition		Phase of Samples
	Temperature(°C)	Time (h)	Temperature(°C)	Time (h)	
a	500	1	–	–	B
b	500	1	550	1	B
c	550	1	600	1	B and M
d	550	1	650	1	B and M
e	550	1	650	5	M
f	550	1	700	5	M

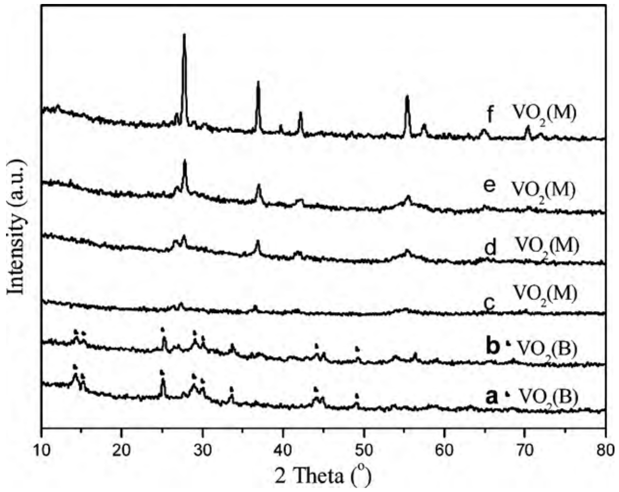

Fig. 3. XRD patterns of the samples obtained at different synthesis conditions.

indicates that there are four elements: tungsten, vanadium, carbon and oxygen. According to the standard binding energy, the peaks at 40.7, 37.2 and 35.0 eV are the binding energy for $W^{6+}{}_{5p3/2}$, $W^{6+}{}_{4f5/2}$ and $W^{6+}{}_{4f7/2}$, respectively [25]. It implies that the valence of tungsten ion in the W-doped VO_2 is +6. Vanadium presents predominantly as V^{4+} with $V_{2p3/2}$ and $V_{2p1/2}$ binding energy at 516.3 eV and 524.0 eV, respectively. The peak at 517.2 eV is $V^{5+}{}_{2p3/2}$ and it means the atmospheric oxidation of a small amount V^{4+} at the surface of sample [25]. The binding energy of O_{1s} appears at 530.0 eV. The peak at 285.1 eV is attributed to C, which is from surface contamination. The XPS compositional results also indicate the phase purity of the W-doped VO_2 sample.

The typical SEM image of the obtained W-doped VO_2 sample is shown in Fig. 5a. It can be seen that sample displays rod-like morphology, which are straight with diameters in the range of 0.1–0.5 μm and lengths in the range of 1–4 μm. Fig. 5b presents a typical energy dispersion spectroscopy (EDS) analysis of W-doped VO_2. It shows that there are V, W and O three elements in sample. The content of W is determined to be 0.71% by quantitative analysis, which is approximately to the doped concentration. The result is in agreement with the XPS data.

To examine the influence of doping W upon the phase Tt of VO_2, the differential scanning calorimetry (DSC) and IR were used to measure the thermal properties of the samples. Fig. 6 shows the typical DSC curves of the W-doped VO_2 with different doping fractions (Table 2). The phase Tt of the undoped VO_2 is 69.5 °C, which is slightly higher than 68 °C reported by Morin [7]. The phase Tt of the doped VO_2 was reduced to 56.2, 43.9 and 37.8 °C when the fraction of W was 0.71, 1.32 and 1.58 mol%, respectively. In our work, the phase Tt decreased about 20 °C with per 1 mol% W doping. This value was close to the phase Tt reduction efficiency studied on bulk single crystal and films [20,21]. The

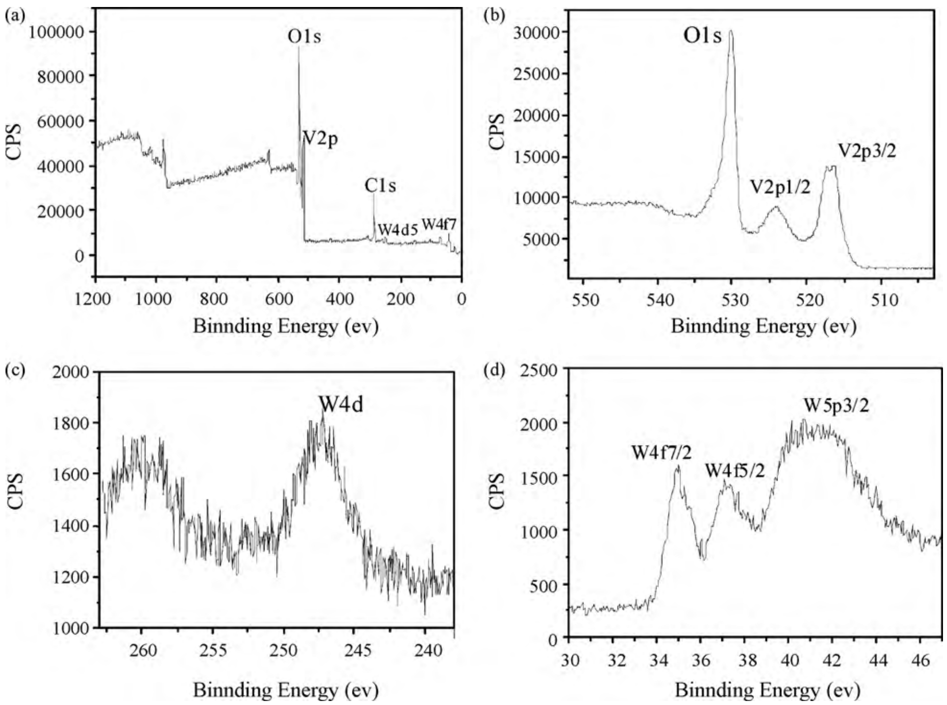

Fig. 4. XPS spectra of the W-doped VO_2.

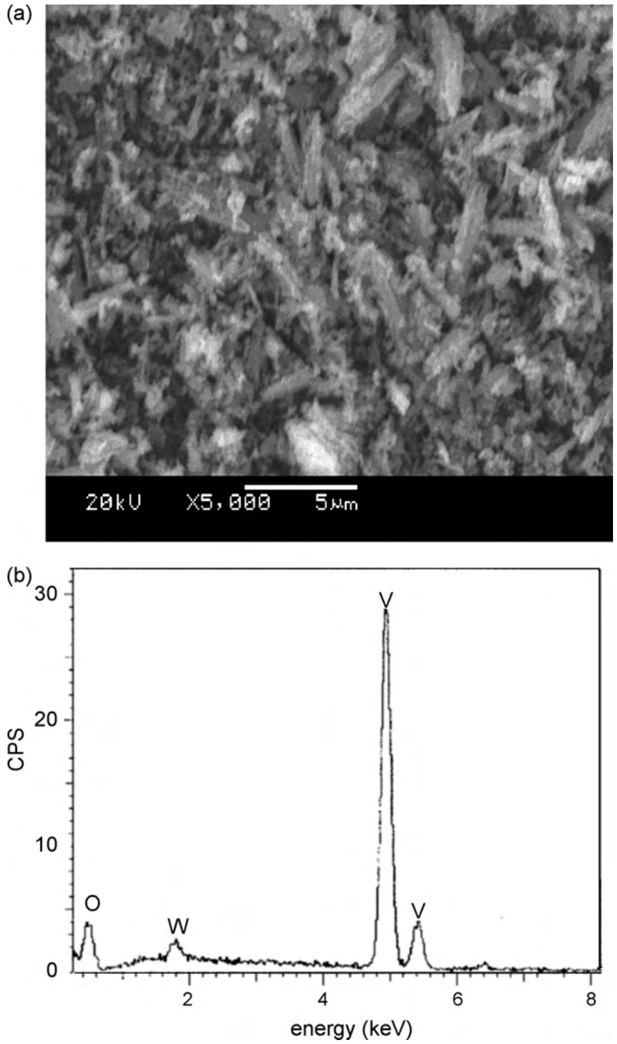

Fig. 5. (a) Typical SEM image and (b) EDS spectrum of the W-doped VO_2.

Table 2
Chemical compositions and phase transition temperature (Tt) of W-doped powders.

Samples	Chemical Compositions	V (wt%)	W (wt%)	O (wt%)	Tt (°C)
a	VO_2	61.45	0	38.55	69.5
b	$V_{0.9929}W_{0.0071}O_2$	60.32	1.56	38.13	56.2
c	$V_{0.9868}W_{0.0132}O_2$	59.38	2.87	37.76	43.9
d	$V_{0.9842}W_{0.0158}O_2$	58.98	3.42	37.60	37.8

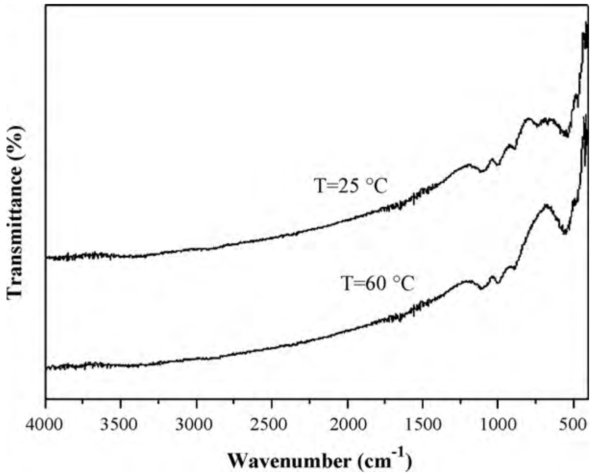

Fig. 7. IR spectra of W-doped VO_2 at 25 °C and 60 °C.

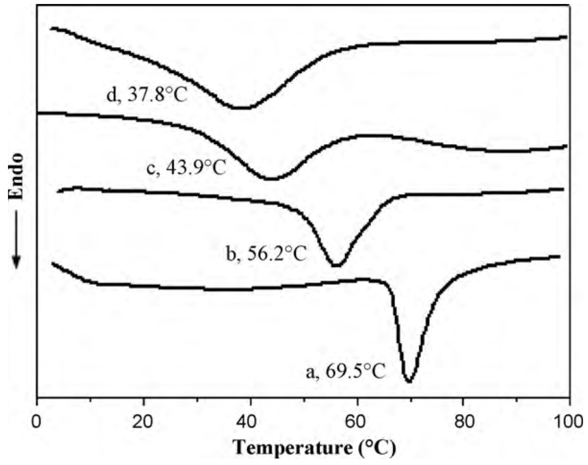

Fig. 6. DSC curves of W-doped VO_2 with different W-doping fractions (mol%): (a) 0%, (b) 0.71%, (c) 1.32%, (d) 1.58%.

results revealed that W atoms could be effectively doped into VO_2 powders and phase Tt of VO_2 can be tuned easily with different W atomic percent. Fig. 7 presents the IR spectra of the resulting W-doped VO_2 at the 25 and 60 °C. Optical switching property of sample is observed according to different IR transmittance below or above the transition temperature (Tt = 56.2 °C) which is similar with VO_2 nano-powders in the literature [22,23]. At 60 °C, the sample exhibited low transmittance in IR spectra. However, at 25 °C, sample exhibited high transmittance. The difference in transmittance resulting from semiconductor-metal transformation suggests that the sample has good thermochromic property.

Up to now, the research about the doped mechanism is still processing. According to the reported models [27–30], W^{6+} penetrates into the crystal lattice of VO_2 and substitutes the V^{4+} ion. For charge compensation, two d-shell electrons from W ion will transfer to the neighboring V ions to form V^{3+}–W^{6+} and V^{3+}–v^{4+} pairs along the *a*-axis of the monoclinic VO_2 cell. Therefore, with the increasing fraction of W^{6+} in the lattice, the loss of homo-polar V^{4+}–V^{4+} bonding becomes more and more obvious, resulting in the semiconductor phase becomes destabilized and the band gap is reduced. This process can decrease the metal-to-semiconductor transition temperature.

4. Conclusions

In summary, a convenient and efficient thermal reduction approach for preparing thermochromic W-doped VO_2 powders has been demonstrated. The experimental results indicate that this process involves an intermediate reduction step, in which metastable VO_2 (B) allotropic phase forms. It suggests that the reduction temperature is the key factor for producing thermochromic VO_2 (M). The required reduction and annealing temperature are 500–550 and 650–700 °C, respectively. The W-doped VO_2 powders display rod-like morphology with diameters in the range of 0.1–0.5 μm. The W doping leads to the tiny change of the host lattice, resulting in the phase transition temperature lowered. When the fraction of W was 1.58 mol%, the phase transition temperature could be reduced to 37.8 °C, suggesting it is beneficial for the development and application of thermochromic materials.

Acknowledgements

Financial support is gratefully acknowledged from National High Technology Research and Development Program of China (863 Program, no. 2008AA03Z306) and Science Research Foundation of Dalian University of Technology.

References

[1] J. Liu, X. Wang, Q. Peng, Y. Li, Adv. Mater. 17 (2005) 764.
[2] H. Serier, M.F. Achard, O. Babot, N. Steunou, J. Maquet, J. Livage, C. Leroy, R. Backov, Adv. Funct. Mater. 16 (2006) 1745.
[3] L. Krusin-Elbaum, D.M. Newns, H. Zeng, V. Derycke, J.Z. Sun, R. Sandstrom, Nature 431 (2004) 672.
[4] C. Karunakaran, S. Senthilvelan, J. Colloid Interface Sci. 289 (2005) 466.
[5] W. Avansi Jr., C. Ribeiro, E.R. Leite, V.R. Mastelaro, Cryst. Growth Des. 9 (2009) 3626.
[6] P. Baum, D.S. Yang, A.H. Zewail, Science 318 (2007) 788.
[7] F.J. Morin, Phys. Rev. Lett. 3 (1959) 34.
[8] A.C. Jones, S. Berweger, J. Wei, D. Cobden, M.B. Raschke, Nano Lett. 10 (2010) 1574.
[9] D. Xiao, K.W. Kim, J.M. Zavada, J. Appl. Phys. 97 (2005) 106102.
[10] J.F. Liu, Q.H. Li, T.H. Wang, D.P. Yu, Y.D. Li, Angew. Chem. 116 (2004) 5158.
[11] M.M. Qazilbash, M. Brehm, B.G. Chae, P.C. Ho, G. Andreev, B.J. Kim, S.J. Yun, A.V. Balatsky, M.B. Maple, F. Keilmann, H.T. Kim, D.N. Basov, Science 318 (2007) 1750.
[12] J. Wei, Z.H. Wang, W. Chen, D.H. Cobden, Nat. Nanotechnol. 4 (2009) 420.
[13] E. Baudrin, G. Sudant, D. Larcher, B. Dunn, J.M. Tarascon, Chem. Mater. 18 (2006) 4369.
[14] G.C. Li, K. Chao, H.R. Peng, K.Z. Chen, Z.K. Zhang, Inorg. Chem. 46 (2007) 5787.
[15] C.Z. Wu, J. Dai, X.D. Zhang, J.L. Yang, F. Qi, C. Gao, Y. Xie, Angew. Chem. 122 (2010) 138.
[16] Q. Su, C.K. Huang, Y. Wang, Y.C. Fan, B.A. Lu, W. Lan, Y.Y. Wang, X.Q. Liu, J. Alloys Compd. 475 (2009) 518.
[17] X.P. Yan, J. Chen, J.M. Liu, P.P. Zhou, X. Liu, Z.X. Su, Mater. Lett. 64 (2010) 278.
[18] J.Q. Shi, S.X. Zhou, B. You, L.M. Wu, Sol. Energy Mater. Sol. Cells 91 (2007) 1856.
[19] T.J. Hanlon, J.A. Coath, M.A. Richardson, Thin Solid Films 436 (2003) 269.
[20] C.X. Cao, Y.F. Gao, H.J. Luo, J. Phys. Chem. C 112 (2008) 18810.
[21] Z.F. Peng, W. Jiang, H. Liu, J. Phys. Chem. C 111 (2007) 1119.
[22] Z.F. Peng, Y. Wang, Y.Y. Du, D. Lu, D.Z. Sun, J. Alloys Compd. 480 (2009) 537.
[23] J. Li, C.Y. Liu, L.J. Ma, J. Solid State Chem. 182 (2009) 2835.
[24] J. Qi, G.L. Ning, Y. Lin, Mater. Res. Bull. 43 (2008) 2300.
[25] J.Z. Yan, Y. Zhang, W.X. Huang, M.G. Tu, Thin Solid Films 516 (2008) 8554.
[26] J.C. Valmatette, J.R. Gavarri, Mater. Sci. Eng. B 54 (1998) 168.
[27] C. Tang, P. Georgopoulos, M.E. Fine, J.B. Cohen, Phys. Rev. B 31 (1985) 1000.
[28] M. Pan, H.M. Zhong, S.W. Wang, J. Liu, Z.F. Li, X.S. Chen, W. Lu, J. Cryst. Growth 265 (2004) 121.
[29] A.R. Begishev, G.B. Galiev, A.S. Ignat'ev, V.G. Mokerov, V.G. Poshin, Sov. Phys. Solid State 20 (1978) 951.
[30] C.H. Griffiths, H.K. Eastwood, J. Appl. Phys. 45 (1974) 2201.